A comparative analysis of differentially expressed genes in rostral and caudal regions after spinal cord injury in rats

https://doi.org/10.4103/1673-5374.336874

Date of submission: August 26, 2021

Date of decision: November 26, 2021

Date of acceptance: December 24, 2021

Date of web publication: February 28, 2022

Xue-Min Cao[#], Sheng-Long Li[#], Yu-Qi Cao, Ye-Hua Lv, Ya-Xian Wang, Bin Yu[*], Chun Yao[*]

From the Contents

Graphical Abstract

The process of comparison of differentially expressed genes in the rostral and caudal regions after spinal cord injury in rats

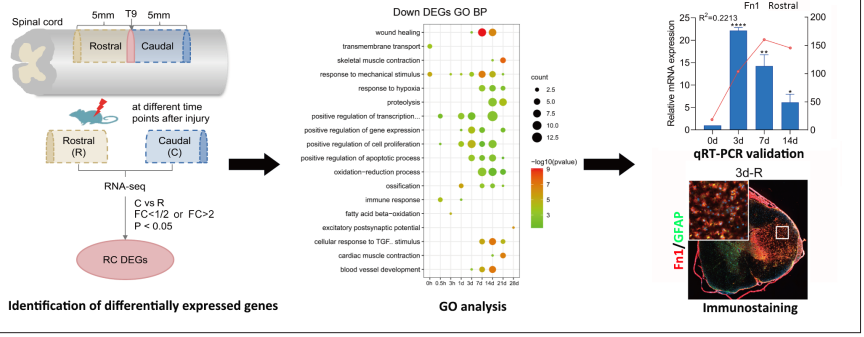

Abstract

The initial mechanical damage of a spinal cord injury (SCI) triggers a progressive secondary injury cascade, which is a complicated process integrating multiple systems and cells. It is crucial to explore the molecular and biological process alterations that occur after SCI for therapy development. The differences between the rostral and caudal regions around an SCI lesion have received little attention. Here, we analyzed the differentially expressed genes between rostral and caudal sites after injury to determine the biological processes in these two segments after SCI. We identified a set of differentially expressed genes, including *Col3a1*, *Col1a1*, *Dcn*, *Fn1*, *Kcnk3*, and *Nrg1*, between rostral and caudal regions at different time points following SCI. Functional enrichment analysis indicated that these genes were involved in response to mechanical stimulus, blood vessel development, and brain development. We then chose *Col3a1*, *Col1a1*, *Dcn*, *Fn1*, *Kcnk3*, and *Nrg1* for quantitative real-time PCR and Fn1 for immunostaining validation. Our results indicate alterations in different biological events enriched in the rostral and caudal lesion areas, providing new insights into the pathology of SCI.

Key Words: biological process; caudal; differentially expressed genes; Gene Ontology; hemisection; immunostaining; Rattus norvegicus; RNA-sequencing; rostral; spinal cord injury

Introduction

Traumatic spinal cord injury (SCI) affects million people worldwide each year, and it can lead to severe nerve dysfunction (Assinck et al., 2017). In the first 2 days (acute phase) after SCI, cell death, inflammatory cell infiltration and hemorrhaging occur. Astrogliosis, fibroblast infiltration, and axon degeneration happen later in the subacute phase (2–14 days). Finally, glial and fibrous scarring restricts axon regeneration and leads to neurological impairments (Ahuja and Fehlings, 2016). Traditional treatments, such as hemodynamic management and surgical decompression, affect neurological outcomes only when administered immediately after acute SCI and provide minor improvements (Squair et al., 2018). The complexity of the pathological mechanisms triggered by SCI contributes to the lack of effective SCI therapies (Telemacque et al., 2020; Zhang et al., 2021). Thus, it is pivotal to better understand the biochemical and cellular events that occur after SCI, which might facilitate the exploration of promising SCI therapies.

The development of transcriptome analysis using microarrays and high-throughput sequencing has provided tremendous information regarding the pathology of SCI from minutes after an injury to the late chronic stage. Using multiple bioinformatic methods, such as time-series expression analysis, differentially expressed gene clustering, or weighted gene coexpression network analysis, researchers have established gene modules corresponding to various pathological events and have identified a set of genes following SCI in mammals (Duan et al., 2015; Jeong et al., 2016; Fink et al., 2017; Squair et al., 2018; Yu et al., 2019).

In a previous study, spinal cord was completely transected at the T9 level with microscissors. Atrophic changes were observed in both the rostral and caudal spinal cord lesion area after SCI. However, the majority of the decreased area in the rostral spinal cord was observed in the white matter, whereas both white and gray matter were decreased in the caudal region, indicating a different injury impact between the rostral and caudal spinal cord (Yokota et al., 2019). However, the pathological and molecular differences between rostral and caudal regions relative to the lesion after SCI have received little attention. Previous studies reported that some proteins, such as glial cell line-derived neurotrophic factor (Zhou et al., 2008; Hara et al., 2012) and phosphorylated calcium/calmodulin-dependent protein kinase II alpha (Song et al., 2009), were expressed in the rostral and caudal regions at different time points and intensity after SCI. Additionally, a proteomic analysis showed that an inflammatory and neurotrophic response occurred regionally between the rostral and caudal segments after acute SCI (Cizkova et al., 2014). However, some studies suggested that the differences between the injury in the rostral and caudal regions were negligible (Duan et al., 2015).

In this study, a rat hemisection SCI model was used for its repeatability and because less loss of innervation can be compensated by sprouting of fibers from the intact side in this model than other models (Kjell and Olson, 2016). Our previous study suggested that the main pathological trends in the rostral and caudal regions were similar to a certain degree (Yu et al., 2019). Previously, we found differentially expressed genes (DEGs) in the rostral and caudal regions compared with a sham group at each time point. In this paper, we compared gene expression in the rostral and caudal regions, and identified DEGs between

Key Laboratory of Neuroregeneration of Jiangsu and Ministry of Education, NMPA Key Laboratory for Research and Evaluation of Tissue Engineering Technology Products, Co-innovation Center of Neuroregeneration, Nantong University, Nantong, Jiangsu Province, China

*Correspondence to: Chun Yao, PhD, yaochun@ntu.edu.cn; Bin Yu, PhD, yubin@ntu.edu.cn.

https://orcid.org/0000-0002-8927-3333 (Bin Yu); https://orcid.org/0000-0002-3706-955X (Chun Yao)

# These authors contributed equally to this paper.

Funding: *This work was supported by Postgraduate Research & Practice Innovation Program of Jiangsu Province, No. KYCX-2065 (to XMC).*

How to cite this article: *Cao XM, Li SL, Cao YQ, Lv YH, Wang YX, Yu B, Yao C (2022) A comparative analysis of differentially expressed genes in rostral and caudal regions after spinal cord injury in rats. Neural Regen Res 17(10):2267-2271.*

the rostral and caudal lesion regions up to 28 days after SCI. Using bioinformatic analysis and molecular validation, we sought to clarify the biological processes and critical genes affected in the rostral and caudal regions.

Materials and Methods

Animal surgery and tissue collection

Twenty-four 6-week-old female Sprague-Dawley rats weighing 200–250 g were anesthetized with an intraperitoneal injection of mixed narcotics (85 mg/kg chloral hydrate, 42 mg/kg magnesium sulfate, and 17 mg/kg sodium pentobarbital; Shanghai Lingfeng Chemical Reagent Co., Ltd, Shanghai, China) and underwent spinal cord T9 hemisection injury with a 15° ophthalmic iris knife on the right side of the spinal cord (Wu et al., 2019; Yu et al., 2019). The animals were kept in a heating blanket to maintain body temperature at 37°C during the surgery. After the surgery, animals were housed in cages at 37°C with five rats per cage on a 12-hour light-dark cycle with free access to food and water. The rats were euthanized and 5-mm-long segments rostral and caudal to the T9 injury site were collected at time points: 0 hours, 3 days, 7 days and 14 days after injury. The animal procedures were approved by the Administration Committee of Experimental Animals of Nantong University, Jiangsu Province, China, and were conducted in accordance with international laws and National Institutes of Health (NIH) policies, including the Care and Use of Laboratory Animals (NIH publication No. 85-23, 1985, revised 1996). This study is reported in accordance with the Animal Research: Reporting of *In Vivo* Experiments 2.0 guidelines (Percie du Sert et al., 2020).

Differentially expressed gene identification

The RNA sequencing (RNA-Seq) data in the rostral and caudal groups at different time points after SCI (0 hours, 0.5 hours, 3 hours, 6 hours, 12 hours, 1 day, 3 days, 7 days, 14 days, 21 days, and 28 days after the injury) were collected in our previous study (Yu et al., 2019) and can be viewed and obtained in NODE (http://www.biosino.org/node; accession: OEP000369). Genes differentially expressed in the caudal group compared with rostral group at different time points were screened and identified with a DESeq package (Shanghai OE Biotech Co., Ltd, Shanghai, China). A negative binomial distribution test was used to test the significance of differences in gene reads number. Genes with $P < 0.05$ and fold change > 2 or fold change < 0.5 were considered differentially expressed.

Bioinformatic analysis

The enriched biological processes associated with downregulated or upregulated DEGs between the rostral and caudal groups at different time points after SCI were identified by gene ontology analysis (Azuaje et al., 2006) using DAVID bioinformatic resources (https://david.ncifcrf.gov/).

RNA isolation and quantitative reverse transcription-PCR

Total RNA was isolated from 5-mm-long segments of the rostral and caudal regions at the indicated time points after SCI using Trizol Reagent (Thermo Fisher Scientific, Waltham, MA, USA). Each time point had three rats in each group. Reverse-transcribed cDNA was synthesized with the Prime-Script RT reagent kit (TaKaRa, Dalian, China). Quantitative real-time PCR (qRT-PCR) was performed with SYBR Premix Ex Taq (TaKaRa) on an ABI StepOne system (Applied Biosystems, Foster City, CA, USA) in triplicate for each sample. The relative expression level was normalized to GAPDH expression and calculated using the $2^{-\Delta\Delta Ct}$ method (Livak and Schmittgen, 2001). The primers used were listed in **Additional Table 1**.

Immunohistochemistry

At 0 days, 3 days, and 7 days after spinal cord hemisection, rats were euthanized by an intraperitoneal injection of mixed narcotics and transcardially perfused with 4% paraformaldehyde. The spinal cord tissue around the lesion (10 mm long) was collected ($n = 3$ for each group). All tissues were transversely sectioned at 20 μm thickness. Sections were immunostained with anti-glial fibrillary acidic protein (GFAP), an astrocyte marker (1:40, chicken, Cat# ab4674, Abcam, Cambridge, USA) and anti-fibronectin (FN1) (1:400, rabbit, Cat# ab2413, Abcam) antibodies overnight at 4°C and incubated with the secondary antibodies: goat anti-chicken Alexa Fluor 488 (1:500, Cat# ab150173, Abcam) and donkey anti-rabbit Alexa Fluor 594 (1:500, Cat# ab150076, Abcam) at room temperature for 2 hours. Finally, the sections were observed under a fluorescence microscope (AxioImager M2, Zeiss, Oberkochen, Germany). Quantification of Fn1 immunostaining (mean integrated optical density, IOD) was performed using Image-Pro Plus 6.0 software (Media Cybernetics, Rockville, MD, USA).

Statistical analysis

All data were presented as the mean ± standard deviation. Statistical comparison was performed with one-way analysis of variance with Dunnett's multiple comparisons test using GraphPad Prism 8 (GraphPad Software, San Diego, CA, USA). P value < 0.05 was considered statistically significant. The correlation coefficients between qRT-PCR and RNA-Seq results were presented as R^2 (coefficient of determination), which were calculated using the Pearson correlation coefficient by Microsoft Excel (2019, Microsoft, Redmond, WA, USA). Biochemical and histological analyses were conducted by researchers blinded to treatment.

Results

Differentially expressed genes between rostral and caudal regions after SCI

In total, 5-mm-long segments in the regions rostral and caudal to the T9 injury site were collected at different time points for RNA-Seq (**Figure 1A**). We compared gene expression between the rostral and caudal groups. Genes with fold change (FC) < 1/2 (caudal *versus* rostral) were considered as downregulated in the caudal group whereas genes with an FC > 2 were considered as upregulated in the caudal group. There was a large number of DEGs (55 genes at 0 hours, 42 genes at 0.5 hours, 45 genes at 3 hours, 34 genes at 6 hours, 26 genes at 12 hours, 50 genes at 1 day, 125 genes at 3 days, 176 genes at 7 days, 230 genes at 14 days, 99 genes at 21 days and 41 genes at 28 days) between the rostral and caudal groups at different time points after SCI, especially after 3 days (**Figure 1B** and **Additional Table 2**).

Biological processes enriched in the rostral and caudal regions

Gene ontology enrichment analysis was performed to identify key biological processes of the DEGs. Immediately after injury at 0.5 hours, downregulated DEGs (FC [caudal *versus* rostral] < 1/2, genes with high expression in the rostral region and low expression in the caudal region) were mainly enriched in immune response. At 1 day after SCI, DEGs were enriched in positive regulation of cell proliferation, which peaked at 3 days. This biological process continued until 14 days. After 3 days, response to mechanical stimulus, blood vessel development, and wound healing were enriched in the rostral region. During the later period (7–28 days) after SCI, biological processes were mainly enriched in cellular response to transforming growth factor-β (TGFβ) stimulus (**Figure 2A** and **Additional Table 3**). In the caudal region, immune response occurred at the early phase at 1 day after SCI. During the period from 3 days to 14 days, upregulated DEGs (FC [caudal *versus* rostral] > 2, genes with high expression in the caudal region and low expression in the rostral region) were enriched in potassium ion transmembrane transport and brain development. After 7 days, DEGs were enriched in biological processes including neuron fate commitment and spinal cord motor neuron cell fate specification in the caudal region compared with the rostral region (**Figure 2B** and **Additional Table 4**).

qRT-PCR validation of key DEGs between the rostral and caudal regions

We then tried to find key DEGs between the rostral and caudal lesion areas after SCI. Genes participating in multiple biological processes are listed in **Table 1**. Among them, *Col3a1*, *Col1a1*, *Dcn*, *Fn1*, *Lox*, *Postn*, *Tnc*, *Isl2*, *Isl1*, *Kcnk3*, and *Nrg1* had significantly different FPKM expression between the rostral and caudal regions at certain time points according to the RNA-Seq data (**Figure 3**). *Col3a1*, *Col1a1*, *Dcn*, *Fn1*, *Lox*, *Postn*, and *Tnc* were more highly expressed in the rostral group, whereas *Isl2*, *Isl1*, *Kcnk3*, and *Nrg1* were highly expressed in the caudal group. We then performed qRT-PCR to validate the mRNA expression changes of these key DEGs with high FPKM expression (**Figure 4**). *Col1a1*, *Col3a1*, *Dcn*, and *Fn1* indeed had an increased expression from 3 days to 14 days after SCI in the rostral region compared with that in the caudal region. And their expression increased with time after SCI. In contrast, expression of *Kcnk3* and *Nrg1* were both decreased in the rostral region and caudal region after SCI. The results of qRT-PCR were mostly consistent with RNA-Seq data.

Table 1 | **Enriched Go terms and genes**

Terms	Genes
Enriched Go Term of Downregulated DEGs in C vs. R	
Blood vessel development	*Agtr1a*, *Col1a1*, *Col3a1*, *Col5a1*, *Gja5*, *Lox*, *Stra6*, *Tbx1*
Cellular response to TGFβ stimulus	*Ankrd1*, *Col1a1*, *Fn1*, *Nox4*, *Postn*, *Wnt10a*, *Wnt2*
Response to mechanical stimulus	*Ankrd23*, *Bglap*, *Cd36*, *Col1a1*, *Col3a1*, *Dcn*, *Fosb*, *Hspa1b*, *Mmp13*, *Ngf*, *Postn*, *Sost*, *Tnc*
Wound healing	*Col1a1*, *Col3a1*, *Dcn*, *Fn1*, *Il24*, *Itga2*, *Lox*, *Postn*, *Serpinb2*, *Tgfb3*, *Tnc*
Enriched Go Term of Upregulated DEGs in C vs. R	
Brain development	*B3gnt5*, *Grhl2*, *Hes5*, *Hmx3*, *Kcnk3*, *Nefh*, *Nrg1*, *Rph3a*, *Slc17a8*
Neuron fate commitment	*Ascl1*, *Gbx1*, *Isl1*, *Isl2*, *Nrg1*
Positive regulation of blood pressure	*Cartpt*, *Glp1r*, *Olr59*, *Uts2*
Potassium ion transmembrane transport	*Htr3a*, *Kcnc3*, *Kcng4*, *Kcnk3*, *Kcnk9*
Spinal cord motor neuron cell fate specification	*Hoxc10*, *Isl1*, *Isl2*, *Mnx1*, *Olig3*

C: Caudal; DEGs: differentially expressed genes; R: rostral. The full names of genes are shown in Additional Table 5.

Fibronectin immunostaining

Using qRT-PCR we confirmed the upregulation of *Col1a1*, *Col3a1*, *Dcn* and *Fn1* in the rostral region compared with the caudal region after SCI. Of those, the expression of Fn1 was increased from 3 days after SCI. Considering the pivotal role of fibronectin (FN1) in treatments for SCI (King et al., 2010; Haggerty et al., 2017), we then chose FN1 for immunostaining validation. Immunostaining assay was performed to detect FN1 expression at 0 days (uninjured), 3 days and 7 days after SCI. As shown in **Figure 5**, FN1 was rarely expressed in the uninjured sham group. However, elevated FN1 expression was induced around the lesion area at 3 days and 7 days after SCI. The immunostaining data were consistent with the RNA-Seq and qRT-PCR results that the Fn1 gene was highly expressed in the rostral region. In addition, we coimmunostained FN1 with GFAP, as it has been reported that FN1 enhances spinal cord astrocyte proliferation (Xia and Zhu, 2014). However, FN1 was mainly expressed in the lesion region and co-expressed slightly with GFAP staining after SCI (**Figure 5**).

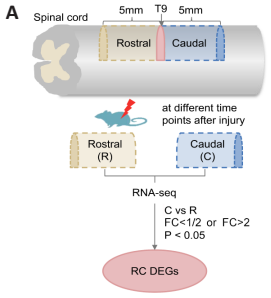

Figure 1 | Identification of differentially expressed genes (DEGs) between the rostral (R) and caudal (C) regions after SCI.

(A) Schematic diagram of spinal cord hemisection, sample groups, RNA-Seq, and DEG identification. As shown in the graph, genes with fold change (FC) (C *vs.* R) < 1/2 (downregulated DEGs) or > 2 (upregulated DEGs), and $P < 0.05$ were considered as DEGs between R and C. (B) The numbers of upregulated and downregulated DEGs between R and C sites at different time points after SCI. SCI: Spinal cord injury.

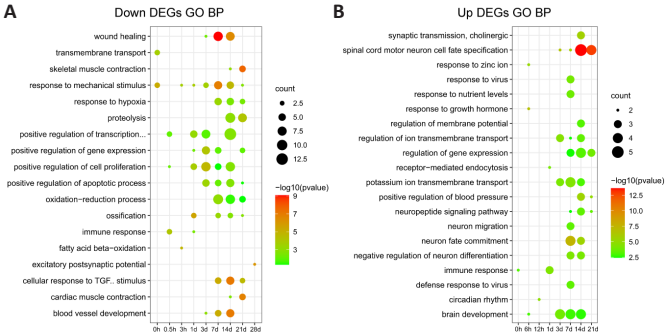

Figure 2 | Enriched Gene Ontology (GO) biological processes of upregulated and downregulated DEGs between the rostral (R) and caudal (C) regions at different time points following SCI.

(A) Enriched GO biological processes (BP) terms of downregulated DEGs, which were upregulated in R relative to C with fold change (FC) (C *vs.* R) < 1/2. (B) Enriched GO BP terms of upregulated DEGs, which were upregulated in C relative to R with FC (C *vs* R) > 2. The color represents −log10 (*P*-value) of each GO term. The circle size indicates gene numbers involved in each GO BP term.

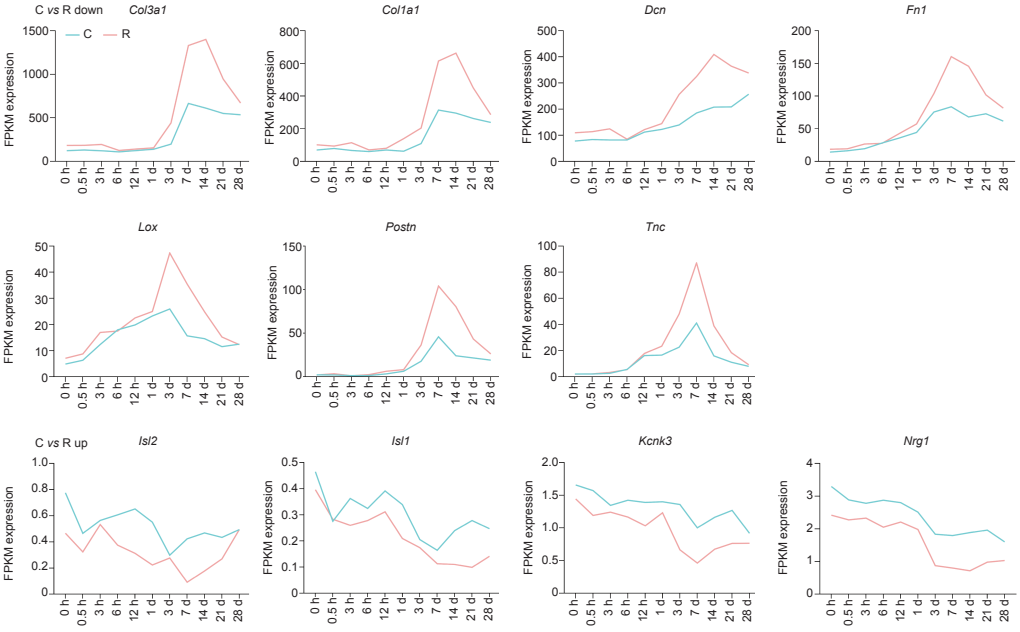

Figure 3 | FPKM expression of key genes in the rostral (R) and caudal (C) regions after SCI according to RNA-Seq data.

The expressions of *Col3a1*, *Col1a1*, *DCN*, *Fn1*, *Lox*, *Postn*, and *Tnc* were upregulated after SCI and were lowlt expressed in the C group compared with the R group. *Isl2*, *Isl1*, *Kcnk3*, and *Nrg1* were downregulated after SCI and were highly expressed in the C group compared with the R group. SCI: Spinal cord injury.

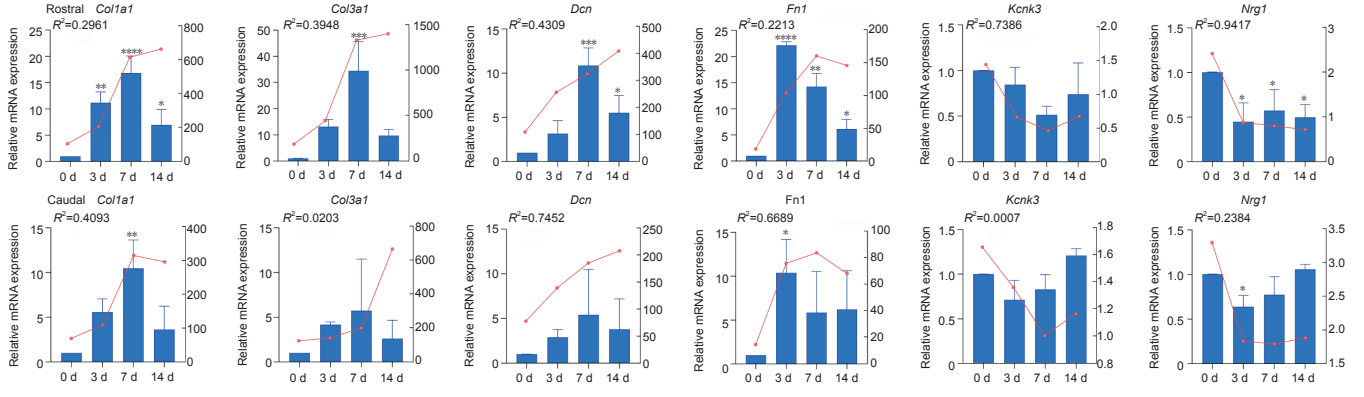

Figure 4 | qRT-PCR validation of selected genes in rostral (R) and caudal (C) regions after SCI.

The blue bar shows the relative mRNA expression of genes at 0 days, 3 days, 7 days, and 14 days after SCI detected by qRT-PCR. The red line above the bar shows the FPKM expression trend of genes by RNA-Seq. $n = 3$ for each group. R^2 represents the correlation coefficient between qRT-PCR validation and RNA-Seq data. *$P < 0.05$, **$P < 0.01$, ***$P < 0.001$, ****$P < 0.0001$. qRT-PCR: Quantitative reverse transcription-PCR; SCI: spinal cord injury.

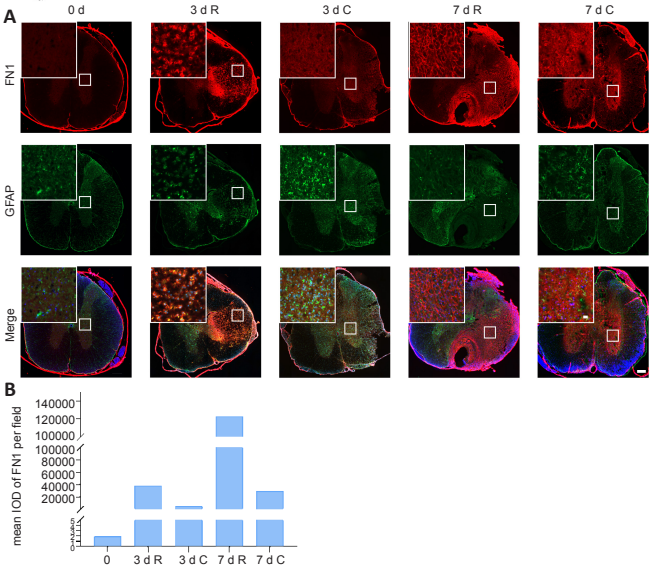

Figure 5 | **Immunostaining of FN1 in the rostral (R) and caudal (C) regions around the SCI lesion.**
(A) Representative images of FN1 (red) and GFAP (green) immunostaining in the spinal cord cross-section at 0 days (uninjured), 3 days and 7 days after SCI. The fluorescence intensity showed the expression level of protein FN1 and GFAP. Spinal cords of uninjured, and R and C regions of 3 days and 7 days were displayed as 0 d, 3 d R, 3 d C, 7 d R and 7 d C, respectively. The nucleus was stained with DAPI (blue). Scale bar: 200 μm. Magnifications of the images in the white squares of the lesion area are shown in the upper left corner. Scale bars: 20 μm. (B) Quantitative result of FN1 (mean IOD). DAPI: 4′,6-Diamidino-2-phenylindole; FN1: fibronectin; GFAP: glial fibrillary acidic protein; IOD: integrated optical density; SCI: spinal cord injury.

Discussion

The differences in the biological processes enriched in the rostral and caudal lesion regions after SCI have not been well studied. In the present study, we identified key biological processes and genes in the rostral and caudal lesion areas (**Figure 6**). At 0.5 hours after SCI, events such as immune response predominated in the rostral region. Response to mechanical stimulus, blood vessel development, and wound healing then followed in the rostral region. Upregulated DEGs in the caudal region versus the rostral region were enriched in potassium ion transmembrane transport and brain development. DEGs were enriched in cellular response to TGFβ stimulus in the rostral region, especially at 14 days, whereas DEGs were enriched in neuron fate commitment and specification in the caudal region. DEGs enriched in blood vessel development were identified in the rostral region during 3–14 days after SCI, suggesting it is in the rostral region that angiogenesis first takes place. This is noteworthy because angiogenesis plays a critical biological role by providing nutritional support and oxygenation for growing tissue after injury (Ng et al., 2011). Furthermore, genes involved in neuron fate and synaptic transmission had more dominant roles in the caudal region compared with the rostral region during the late period, indicating that these processes satisfy the high demands for energy and ion homeostasis necessary for tissue regeneration (Cai et al., 2011). These results suggest that the rostral and caudal regions to the lesion may undergo different biological processes after SCI.

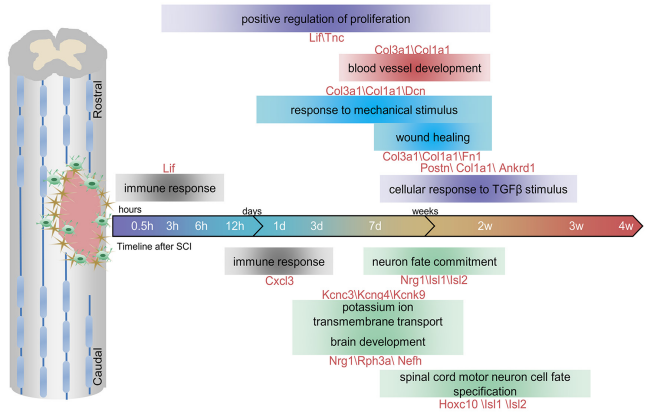

Figure 6 | **Schematic of the major biological processes and genes in rostral (R) and caudal (C) regions at different time points after spinal cord injury.**
We identified key biological processes and genes in the R and C lesion areas. Blood vessel development, cellular response to transforming growth factor-β, response to mechanical stimulus, positive regulation of proliferation and wound healing were enriched in the rostral region. Brain development, neuron fate commitment, potassium ion transmembrane transport and spinal cord motor neuron cell fate specification were enriched in the caudal region. The genes shown below or above the biological processes were involved in the corresponding biological processes. The full names are shown in Additional Table 5.

We identified DEGs involved in multiple biological processes that differed between the rostral and caudal regions at certain time points. *Col1a1* and *Col3a1* encode type I and III collagen in connective tissues (Li et al., 2016). In addition, *Col1a1* and *Col3a1* are upregulated in cancers and are correlated with tumor progression and metastasis, suggesting the involvement of these two genes in cell proliferation, migration, and focal adhesion (Kuivaniemi and Tromp, 2019; Ma et al., 2019). Decorin (*Dcn*) plays a crucial role in the injured spinal cord by inhibiting scar formation and inflammation, promoting axon regrowth (Davies et al., 2004; Minor et al., 2008). Our results showed that these genes involved in wound healing and response to mechanical stimulus were mainly enriched in the rostral region of the injured spinal cord. Neuregulin-1 (*Nrg1*), a member of the neuregulin family, plays a predominant role in neural circuitry assembly, myelination, and synaptic plasticity in the central nervous system (Mei and Nave, 2014). Previous research demonstrated that *Nrg1* was dysregulated dramatically and permanently after SCI (Gauthier et al., 2013), which is consistent with our data. *Kcnk3* encodes potassium channel proteins and is also expressed in the central nervous system, including in motor neurons (Talley et al., 2001; Berg et al., 2004). *Kcnk3* is neuroprotective and plays a critical role in neurodegeneration and neuronal excitability (Ehling et al., 2015). We found that the expressions of DEGs that were upregulated in caudal *versus* rostral regions decreased with time after SCI both in the rostral and caudal regions. The decreased expression of *Nrg1* and *Kcnk3*, which were enriched in neuron development and ion transport, in the rostral region *versus* the caudal region suggests that SCI-induced neuron dysfunction was severe in the rostral region.

Our results indicated that *Fn1* was also upregulated and highly expressed in the rostral region after SCI. FN1 is an extracellular matrix protein that has multiple effects on wound healing (Patten and Wang, 2021). On the one hand, FN1 is a growth permissive and neuroprotective substrate for nerve repair by promoting cell adhesion and sequestering nutrients and growth factors (Haggerty et al., 2017). FN1 administration can also decrease inflammatory cell invasion and blood-spinal cord barrier breakdown (Lin et al., 2012). On the other hand, the fibrotic scar formed by FN1 at the lesion area after SCI inhibits axon regeneration (Zhu et al., 2015; Cooper et al., 2018). Recently, researchers found that after SCI, a subset of microglia highly express FN1 to facilitate scar-free wound healing (Li et al., 2020). Loss of FN1 in microglia resulted in increased GFAP$^+$ astrocytes in the lesion site (Li et al., 2020). Consistently, our results showed that FN1 was rarely expressed in the GFAP-positive astrocytes after SCI.

Limitations

In this study, we performed qRT-PCR and immunostaining to validate the expression changes of DEGs. We did not conduct deep exploration on the function of these genes *in vitro* or *in vivo*. The differences in the enriched processes and specific genes between the rostral and caudal segments after SCI have not been fully explored in the present study. Recently, the development of single-cell sequencing has provided new insights for the investigation of the microenvironment after SCI, which we could adopt for exploration in the future (Sathyamurthy et al., 2018). In addition, multi-omics analyses integrating genomics, transcriptomics, proteomics, and metabolomics should be applied to explore the complicated microenvironment after SCI. In the future, we will perform additional experiments to detect the detailed functions of these DEGs in rostral and caudal regions in effort to develop new effective therapeutic targets for SCI.

Conclusion

In this study, we investigated the differences in biological processes and expression module of genes between the rostral and caudal regions after SCI in rats. Using bioinformatic analysis and molecular validation, we identified the main biological processes and key DEGs in the rostral and caudal regions. This study on the differences between the rostral and caudal regions would help to understand the recovery of spinal cord injury.

Author contributions: *CY and BY conceived and designed the experiments. XMC, SLL, YQC, YHL and YXW performed the experiments. XMC and CY analyzed the data. CY and XMC wrote the paper. CY and BY revised the manuscript. All authors read and approved the final manuscript.*
Conflicts of interest: *The authors declare no competing interests.*
Editor note: BY is an Editorial Board member of Neural Regeneration Research. He was blinded from reviewing or making decisions on the manuscript. The article was subject to the journal's standard procedures, with peer review handled independently of this Editorial Board member and their research groups.
Availability of data and materials: *All data generated or analyzed during this study are included in this published article and its supplementary information files.*

Additional files:
Additional Table 1: *qRT-PCR pimers of key differentially expressed genes between rostral and cadual regions after spinal cord injury.*
Additional Table 2: *Differentially expressed genes after spinal cord injury at*

different time points between rostral and caudal groups.
Additional Table 3: *Enriched GO terms of differentially expressed genes with fold change < 1/2, genes highly-expressed in the rostral region around SCI lesion.*
Additional Table 4: *Enriched GO terms of differentially expressed genes with fold change > 2, genes highly-expressed in the caudal region around SCI lesion.*
Additional Table 5: *Abbreviations and full names of genes in Table 1 and Figure 6.*

References

Ahuja CS, Fehlings M (2016) Concise review: bridging the gap: novel neuroregenerative and neuroprotective strategies in spinal cord injury. Stem Cells Transl Med 5:914-924.

Assinck P, Duncan GJ, Hilton BJ, Plemel JR, Tetzlaff W (2017) Cell transplantation therapy for spinal cord injury. Nat Neurosci 20:637-647.

Azuaje F, Al-Shahrour F, Dopazo J (2006) Ontology-driven approaches to analyzing data in functional genomics. Methods Mol Biol 316:67-86.

Berg AP, Talley EM, Manger JP, Bayliss DA (2004) Motoneurons express heteromeric TWIK-related acid-sensitive K+ (TASK) channels containing TASK-1 (KCNK3) and TASK-3 (KCNK9) subunits. J Neurosci 24:6693-6702.

Cai Q, Davis ML, Sheng ZH (2011) Regulation of axonal mitochondrial transport and its impact on synaptic transmission. Neurosci Res 70:9-15.

Cizkova D, Le Marrec-Croq F, Franck J, Slovinska L, Grulova I, Devaux S, Lefebvre C, Fournier I, Salzet M (2014) Alterations of protein composition along the rostro-caudal axis after spinal cord injury: proteomic, in vitro and in vivo analyses. Front Cell Neurosci 8:105.

Cooper JG, Jeong SJ, McGuire TL, Sharma S, Wang W, Bhattacharyya S, Varga J, Kessler JA (2018) Fibronectin EDA forms the chronic fibrotic scar after contusive spinal cord injury. Neurobiol Dis 116:60-68.

Davies JE, Tang XF, Denning JW, Archibald SJ, Davies SJA (2004) Decorin suppresses neurocan, brevican, phosphacan and NG2 expression and promotes axon growth across adult rat spinal cord injuries. Eur J Neurosci 19:1226-1242.

Duan H, Ge W, Zhang A, Xi Y, Chen Z, Luo D, Cheng Y, Fan KS, Horvath S, Sofroniew MV, Cheng L, Yang Z, Sun YE, Li X (2015) Transcriptome analyses reveal molecular mechanisms underlying functional recovery after spinal cord injury. Proc Natl Acad Sci U S A 112:13360-13365.

Ehling P, Cerina M, Budde T, Meuth SG, Bittner S (2015) The CNS under pathophysiologic attack-examining the role of K-2P channels. Pflug Arch Eur J Phy 467:959-972.

Fink KL, Lopez-Giraldez F, Kim IJ, Strittmatter SM, Cafferty WBJ (2017) Identification of Intrinsic Axon Growth Modulators for Intact CNS Neurons after Injury. Cell Rep 18:2687-2701.

Gauthier MK, Kosciuczyk K, Tapley L, Karimi-Abdolrezaee S (2013) Dysregulation of the neuregulin-1-ErbB network modulates endogenous oligodendrocyte differentiation and preservation after spinal cord injury. Eur J Neurosci 38:2693-2715.

Haggerty AE, Marlow MM, Oudega M (2017) Extracellular matrix components as therapeutics for spinal cord injury. Neurosci Lett 652:50-55.

Hara T, Fukumitsu H, Soumiya H, Furukawa Y, Furukawa S (2012) Injury-induced accumulation of glial cell line-derived neurotrophic factor in the rostral part of the injured rat spinal cord. Int J Mol Sci 13:13484-13500.

Jeong H, Na YJ, Lee K, Kim YH, Lee Y, Kang M, Jiang BC, Yeom YI, Wu LJ, Gao YJ, Kim J, Oh SB (2016) High-resolution transcriptome analysis reveals neuropathic pain gene-expression signatures in spinal microglia after nerve injury. Pain 157:964-976.

King VR, Hewazy D, Alovskaya A, Phillips JB, Brown RA, Priestley JV (2010) The neuroprotective effects of fibronectin mats and fibronectin peptides following spinal cord injury in the rat. Neuroscience 168:523-530.

Kjell J, Olson L (2016) Rat models of spinal cord injury: from pathology to potential therapies. Dis Model Mech 9:1125-1137.

Kuivaniemi H, Tromp G (2019) Type III collagen (COL3A1): Gene and protein structure, tissue distribution, and associated diseases. Gene 707:151-171.

Li J, Ding YM, Li AQ (2016) Identification of COL1A1 and COL1A2 as candidate prognostic factors in gastric cancer. World J Surg Oncol 14:297.

Li Y, He X, Kawaguchi R, Zhang Y, Wang Q, Monavarfeshani A, Yang Z, Chen B, Shi Z, Meng H, Zhou S, Zhu J, Jacobi A, Swarup V, Popovich PG, Geschwind DH, He Z (2020) Microglia-organized scar-free spinal cord repair in neonatal mice. Nature 587:613-618.

Lin CY, Lee YS, Lin VW, Silver J (2012) Fibronectin inhibits chronic pain development after spinal cord injury. J Neurotraum 29:589-599.

Livak KJ, Schmittgen TD (2001) Analysis of relative gene expression data using real-time quantitative PCR and the 2(-Delta Delta C(T)) method. Methods 25:402-408.

Ma HP, Chang HL, Bamodu OA, Yadav VK, Huang TY, Wu ATH, Yeh CT, Tsai SH, Lee WH (2019) Collagen 1A1 (COL1A1) is a reliable biomarker and putative therapeutic target for hepatocellular carcinogenesis and metastasis. Cancers (Basel) 11:786.

Mei L, Nave KA (2014) Neuregulin-ERBB signaling in the nervous system and neuropsychiatric diseases. Neuron 83:27-49.

Minor K, Tang XF, Kahrilas G, Archibald SJ, Davies JE, Davies SJ (2008) Decorin promotes robust axon growth on inhibitory CSPGs and myelin via a direct effect on neurons. Neurobiol Dis 32:88-95.

Ng MT, Stammers AT, Kwon BK (2011) Vascular disruption and the role of angiogenic proteins after spinal cord injury. Transl Stroke Res 2:474-491.

Patten J, Wang K (2021) Fibronectin in development and wound healing. Adv Drug Del Rev 170:353-368.

Percie du Sert N, Hurst V, Ahluwalia A, Alam S, Avey MT, Baker M, Browne WJ, Clark A, Cuthill IC, Dirnagl U, Emerson M, Garner P, Holgate ST, Howells DW, Karp NA, Lazic SE, Lidster K, MacCallum CJ, Macleod M, Pearl EJ, et al. (2020) The ARRIVE guidelines 2.0: Updated guidelines for reporting animal research. PLoS Biol 18:e3000410.

Sathyamurthy A, Johnson KR, Matson KJE, Dobrott CI, Li L, Ryba AR, Bergman TB, Kelly MC, Kelley MW, Levine AJ (2018) Massively parallel single nucleus transcriptional profiling defines spinal cord neurons and their activity during behavior. Cell Rep 22:2216-2225.

Song MS, Seo HS, Yang M, Kim JS, Kim SH, Kim JC, Wang H, Sim KB, Kim H, Shin T, Moon C (2009) Activation of Ca2+/calmodulin-dependent protein kinase II alpha in the spinal cords of rats with clip compression injury. Brain Res 1271:114-120.

Squair JW, Tigchelaar S, Moon KM, Liu J, Tetzlaff W, Kwon BK, Krassioukov AV, West CR, Foster LJ, Skinnider MA (2018) Integrated systems analysis reveals conserved gene networks underlying response to spinal cord injury. Elife 7:e39188.

Talley EM, Solorzano G, Lei Q, Kim D, Bayliss DA (2001) Cns distribution of members of the two-pore-domain (KCNK) potassium channel family. J Neurosci 21:7491-7505.

Telemacque D, Zhu FZ, Ren ZW, Chen KF, Drepaul D, Yao S, Yang F, Qu YZ, Sun TF, Guo XD (2020) Effects of durotomy versus myelotomy in the repair of spinal cord injury. Neural Regen Res 15:1814-1820.

Wu RH, Mao SS, Wang YX, Zhou SS, Liu Y, Liu M, Gu XS, Yu B (2019) Differential circular RNA expression profiles following spinal cord injury in rats: a temporal and experimental analysis. Front Neurosci 13:1303.

Xia M, Zhu Y (2014) Fibronectin enhances spinal cord astrocyte proliferation by elevating P2Y1 receptor expression. J Neurosci Res 92:1078-1090.

Yokota K, Kubota K, Kobayakawa K, Saito T, Hara M, Kijima K, Maeda T, Katoh H, Ohkawa Y, Nakashima Y, Okada S (2019) Pathological changes of distal motor neurons after complete spinal cord injury. Mol Brain 12:4.

Yu B, Yao C, Wang Y, Mao S, Wang Y, Wu R, Feng W, Chen Y, Yang J, Xue C, Liu D, Ding F, Gu X (2019) The landscape of gene expression and molecular regulation following spinal cord hemisection in rats. Front Mol Neurosci 12:287.

Zhang LJ, Chen Y, Wang LX, Zhuang XQ, Xia HC (2021) Identification of potential oxidative stress biomarkers for spinal cord injury in erythrocytes using mass spectrometry. Neural Regen Res 16:1294-1301.

Zhou HL, Yang HJ, Li YM, Wang Y, Yan L, Guo XL, Ba YC, Liu S, Wang TH (2008) Changes in Glial cell line-derived neurotrophic factor expression in the rostral and caudal stumps of the transected adult rat spinal cord. Neurochem Res 33:927-937.

Zhu Y, Soderblom C, Trojanowsky M, Lee DH, Lee JK (2015) Fibronectin matrix assembly after spinal cord injury. J Neurotrauma 32:1158-1167.

C-Editor: Zhao M; S-Editor: Li CH; L-Editors: Li CH, Song LP; T-Editor: Jia Y

Additional Table 1 qRT-PCR pimers of key differentially expressed genes between rostral and cadual regions after spinal cord injury

Gene	GenBank	Primer sequences	Size (bp)
Col3a1	NM_032085.1	F:5-AGGGCAGGGAACAACTGATG-3	115
		R:5-GGTCCCACATTGCACAAAGC-3	
Col1a1	NM_053304.1	F:5-TGGCAACCTCAAGAAGTCCC-3	93
		R:5-ACAAGCGTGCTGTAGGTGAA-3	
Fn1	NM_019143.2	F:5-CTGGTTACCCTTCCACACCC-3	84
		R:5-GGTGACGAAGGGGGTCTTTT-3	
Nrg1	NM_001271118.1	F:5-TCCTCTAAGCAGACACCAGC-3	122
		R:AAGAAGGCAGGGGACCAAAA-3	
Dcn	NM_024129.1	F:5-ACCCGGATTAAAAGGTGGTG-3	78
		R:AGACTTGCGCCAGAAGGAAT-3	
Kcnk3	NM_033376.2	F:5-CGCATCAACACCTTCGTGAG-3	107
		R:GACACGAAACCGATGAGCAC-3	

Additional Table 3 Enriched GO terms of differentially expressed genes with fold change < 1/2, genes high-expressed in the rostral region around SCI lesion

Time	Term	Pval	Gene
0.5h	immune response	8.12177E-05	Lif; Lax1; Ccr7
0.5h	positive regulation of cell proliferation	0.007833031	Lif; Wnt10b
0.5h	positive regulation of transcription	0.009456794	Lif; Wnt10b; Mef2b
0h	response to mechanical stimulus	5.93555E-06	Bglap; Cd36; Ankrd23
0h	transmembrane transport	0.000210238	Slc6a4; Aspn; Slc1a7
12h	protein heterooligomerization	5.61952E-06	Scube3; Chrnb3
14d	blood vessel development	8.89E-08	Stra6;Tbx1; Col3a1; Col1a1; Col5a1; Gja5
14d	cardiac muscle contraction	0.002714188	Csrp3; Tnni1
14d	cellular response to TGFβ stimulus	7.80401E-08	Fn1; Nox4; Postn; Ankrd1; Wnt2; Col1a1
14d	ossification	0.002071791	Fn1;Col1a1; Col5a2
14d	oxidation-reduction process	0.031411951	Nox4; Dio2; Aldh1a3; Cyp26a1; Duox1; Pxdn; Cyp4b1; Cyp4f37
14d	positive regulation of apoptotic process	0.001993043	Sfrp4; Nox4; Aldh1a3; Ankrd1; Tgfb3;Igfbp3
14d	positive regulation of cell proliferation	0.002087715	Fn1; Fgf5; Il11; Tbx1; Il31ra; Wnt2; Btc; Tnc
14d	positive regulation of transcription	0.002029382	Gata6; Il11; Meox2; Arntl2; E2f7; Tbx1; Pax9; Lum; Ankrd1; Wnt2; Csrp3; Meox1; Plagl1
14d	proteolysis	0.001171872	Htra3; Dpep2; Anpep; Tmprss11f; F7; Fap; Mmp2; Cfi; Pi15
14d	response to hypoxia	0.003240466	Serpina1; Nox4; Postn; Tgfb3; Mmp2
14d	response to mechanical stimulus	2.02755E-05	Postn; Col3a1;Col1a1; Tnc; Dcn
14d	skeletal muscle contraction	0.000889596	Tnni1; Tnnt3
14d	wound healing	3.22664E-07	Fn1; Postn; Tgfb3; Col3a1;Col1a1; Tnc; Dcn
1d	immune response	0.003524026	Lif; Prg4
1d	ossification	3.24848E-06	Dmp1; Runx2; Sost
1d	positive regulation of cell proliferation	0.000174437	Il11; Lif; Btc; Runx2
1d	positive regulation of gene expression	0.005565439	Lif; Runx2
1d	positive regulation of transcription	0.000679914	Il11; Lif; Ikzf3; Ankrd1; Runx2
1d	response to mechanical stimulus	0.000164895	Hspa1a; Sost
21d	cardiac muscle contraction	1.59498E-07	Actc1; Myh7; Tnni3; Tnni1
21d	cellular response to TGFβ stimulus	2.2742E-05	Postn; Wnt10a; Ankrd1
21d	ossification	0.001848961	Col2a1; Sost
21d	oxidation-reduction process	0.047033426	LOC688778; Hsd11b2; Cyp1a1; Cyp4b1
21d	positive regulation of apoptotic process	0.045428848	Sfrp4; Ankrd1
21d	positive regulation of gene expression	0.010514083	Sfrp4; Wnt10a; Actc1
21d	proteolysis	7.61308E-05	Mmp3; Capn13; Mmp10; Adamts18; Tmprss11f; Fap; Adamts16
21d	response to hypoxia	0.004033166	Postn; Hsd11b2; Cyp1a1

21d	response to mechanical stimulus	0.002057169	Postn; Sost
21d	skeletal muscle contraction	2.1567E-08	Myh3; Myh7; Tnni3; Tnni1
28d	excitatory postsynaptic potential	7.11885E-07	Ghrl; Slc17a7
3d	blood vessel development	0.001091059	Agtr1a; Col3a1
3d	positive regulation of apoptotic process	0.000381421	Sfrp2; Sfrp4; Wnt11; Ankrd1; Hmga2
3d	positive regulation of cell proliferation	2.00273E-05	Sfrp2; Fgf5; Il11; Ngf; Agtr1a; Btc; Hmga2; Tnc
3d	positive regulation of gene expression	7.24941E-05	Apob; Sfrp4; Ngf; Wnt11; Hmga2; Tnc
3d	positive regulation of transcription	0.012859127	Sfrp2; Il11; Hjv; Lum; Ankrd1; Six1; Hmga2
3d	response to mechanical stimulus	0.000236956	Ngf; Col3a1; Tnc
3d	wound healing	0.005492498	Col3a1; Tnc
3h	fatty acid beta-oxidation	1.59562E-05	Acox2; Echs1
3h	response to mechanical stimulus	0.000206533	Hspa1a; Mmp13
7d	blood vessel development	6.17E-06	Lox; Agtr1a; Col3a1; Col1a1
7d	cellular response to TGFβ stimulus	5.62815E-06	Nox4; Postn; Ankrd1;Col1a1
7d	ossification	0.000539876	Mmp9;Col1a1; Mmp13
7d	oxidation-reduction process	0.000917526	Nox4; Duox2; Loxl4; Lox; Dio2; Aldh1l2; Plod2; Cyp4b1; Rn50_10_0892.1
7d	positive regulation of apoptotic process	0.007783141	Sfrp4; Nox4; Mmp9; Ankrd1
7d	positive regulation of cell proliferation	0.046469561	Il11; Agtr1a;Il24; Tnc
7d	positive regulation of gene expression	0.010370091	Sfrp4; Stap1; Slc26a9; Tnc
7d	response to hypoxia	0.00050254	Nox4; Postn; Plod2; Itga2; Mmp13
7d	response to mechanical stimulus	1.21134E-07	Postn; Col3a1;Col1a1; Fosb; Tnc; Mmp13
7d	wound healing	8.21364E-10	Postn; Lox;Il24; Col3a1;Col1a1; Itga2; Tnc; Serpinb2

Additional Table 4 Enriched GO terms of differentially expressed genes with fold change >2, genes high-expressed in the caudal region around SCI lesion

Time	Term	Pval	Gene
0h	immune response	0.000679073	Cxcl3; RT1-CE3
12h	circadian rhythm	1.79892E-05	Slc9a3; Mttp
14d	brain development	0.002331847	Nrg1; Grhl2; Hes5; Nefh
14d	negative regulation of neuron differentiation	8.95208E-05	Hes5; Isl1; Isl2
14d	neuron fate commitment	3.24848E-06	Nrg1; Isl1; Isl2
14d	neuropeptide signaling pathway	0.000385095	RGD1560028; Gpr139; Cartpt
14d	positive regulation of blood pressure	3.24848E-06	Glp1r; Uts2; Cartpt
14d	potassium ion transmembrane transport	0.000909721	Kcng4; Htr3a; Kcnk9
14d	regulation of gene expression	0.000602612	Grhl2; Hoxd9;Olig3; Isl1
14d	regulation of ion transmembrane transport	0.000352014	Kcng4; Kcnj14; Kcnk9
14d	regulation of membrane potential	0.000631874	Htr3a; Chrna3; Tafa4
14d	spinal cord motor neuron cell fate specification	2.28322E-14	Mnx1; Olig3; Isl1; Hoxc10; Isl2
14d	synaptic transmission, cholinergic	1.94163E-06	Slc5a7; Chrm2; Chrna3
1d	immune response	5.22633E-05	RT1-CE5; Sbspon; LOC100910650
1d	receptor-mediated endocytosis	0.000101598	Sbspon; LOC100910650
21d	neuropeptide signaling pathway	0.0003232	Nppa; Cartpt
21d	positive regulation of blood pressure	8.74857E-06	Olr59; Cartpt
21d	regulation of gene expression	0.000139457	Hoxd9; Olig3; Isl1
21d	spinal cord motor neuron cell fate specification	1.38634E-13	Mnx1; Olig3; Isl1; Hoxc10
3d	brain development	0.000124833	Nrg1; Rph3a; Slc17a8;Nefh
3d	potassium ion transmembrane transport	7.90703E-05	Kcnc3; Kcng4; Kcnk9
3d	regulation of ion transmembrane transport	2.95331E-05	Kcnc3; Kcng4; Kcnk9
3d	spinal cord motor neuron cell fate specification	3.06374E-07	Mnx1; Hoxc10
6h	brain development	0.001129211	B3gnt5; Hmx3
6h	response to growth hormone	1.77991E-07	F7; Cps1
6h	response to zinc ion	7.55084E-06	Pln; Cps1
7d	brain development	0.001452408	Nrg1; Rph3a; Nefh ; Kcnk3
7d	defense response to virus	0.000389349	Isg15; Ifit3; Rsad2
7d	negative regulation of neuron differentiation	5.89243E-05	Ascl1; Tlx3; Isl2
7d	neuron fate commitment	3.14616E-08	Nrg1; Ascl1; Gbx1; Isl2
7d	neuron migration	0.000421108	Ascl1; Tlx3; Cdk5r2
7d	neuropeptide signaling pathway	0.003628112	Nmu; RGD1560028
7d	potassium ion transmembrane transport	4.24864E-05	Kcnc3; Kcng4; Htr3a; Kcnk3

7d	regulation of gene expression	0.00329736	Ascl1; Hoxd9; Phlda2
7d	regulation of ion transmembrane transport	0.003395197	Kcnc3;Kcng4
7d	response to nutrient levels	0.00016692	Sds; Gc; Fgf21
7d	response to virus	0.000102913	Ifit3; Rsad2; Batf3
7d	spinal cord motor neuron cell fate specification	1.51865E-06	Hoxc10; Isl2

Additional Table 5 Abbreviation and full name of genes in Table 1

Abbreviation	Full name
Agtr1a	Angiotensin II Receptor Type 1
Ankrd1	Ankyrin Repeat Domain 1
Ankrd23	Ankyrin Repeat Domain 23
Ascl1	Achaete-Scute Family BHLH Transcription Factor 1
B3gnt5	UDP-GlcNAc:BetaGal Beta-1,3-N-Acetylglucosaminyltransferase 5
Bglap	Bone Gamma-Carboxyglutamate Protein
Cartpt	CART Prepropeptide
Cd36	CD36 Molecule
Col1a1	Collagen Type I Alpha 1 Chain
Col3a1	Collagen Type III Alpha 1 Chain
Col5a1	Collagen Type V Alpha 1 Chain
Dcn	Decorin
Fn1	Fibronectin 1
Fosb	FosB Proto-Oncogene, AP-1 Transcription Factor Subunit
Gbx1	Gastrulation Brain Homeobox 1
Gja5	Gap Junction Protein Alpha 5
Glp1r	Glucagon Like Peptide 1 Receptor
Grhl2	Grainyhead Like Transcription Factor 2
Hes5	Hes Family BHLH Transcription Factor 5
Hmx3	H6 Family Homeobox 3
Hoxc10	Homeobox C10
Hspa1b	Heat Shock Protein Family A (Hsp70) Member 1B
Htr3a	5-Hydroxytryptamine Receptor 3A
Il24	Interleukin 24
Isl1	ISL LIM Homeobox 1
Isl2	ISL LIM Homeobox 2
Itga2	Integrin Subunit Alpha 2
Kcnc3	Potassium Voltage-Gated Channel Subfamily C Member 3
Kcng4	Potassium Voltage-Gated Channel Modifier Subfamily G Member 4
Kcnk3	Potassium Two Pore Domain Channel Subfamily K Member 3
Kcnk9	Potassium Two Pore Domain Channel Subfamily K Member 9
Lox	Lysyl Oxidase
Mmp13	Matrix Metallopeptidase 13
Mnx1	Motor Neuron And Pancreas Homeobox 1
Nefh	Neurofilament Heavy Chain
Ngf	Nerve Growth Factor
Nox4	Fibronectin 1NADPH Oxidase 4
Nrg1	Neuregulin 1
Olig3	Oligodendrocyte Transcription Factor 3
Olr59	olfactory receptor 59
Postn	Periostin
Rph3a	Rabphilin 3A
Serpinb2	Serpin Family B Member 2
Slc17a8	Solute Carrier Family 17 Member 8
Sost	Sclerostin
Stra6	Signaling Receptor And Transporter Of Retinol STRA6
Tbx1	T-Box Transcription Factor 1
Tgfb3	Transforming Growth Factor Beta 3
Tnc	Tenascin C
Uts2	Urotensin 2
Wnt10a	Wnt Family Member 10A
Wnt2	Wnt Family Member 2